Supplementary Material

Switching of INCENP paralogs controls transitions in mitotic chromosomal passenger complex functions

Feng et al.

Figure S1. **Temporal deposition of major histone H3 posttranslational phosphorylation modifications on *O. dioica* chromosomes during mitosis.** H3pS10 emerged on chromosome arms at early prophase, increased in intensity as mitosis progressed, peaked at metaphase and was no longer detected in telophase. H3pS28 appeared on centromeres at late prophase, peaked at metaphase and disappeared at telophase. H3pT11 appeared on centromeres at early prophase, and disappeared prior to anaphase. H3pT3 appeared on centromeres at late prophase, peaked at metaphase and disappeared at the onset of anaphase. Bar, 3 μm.

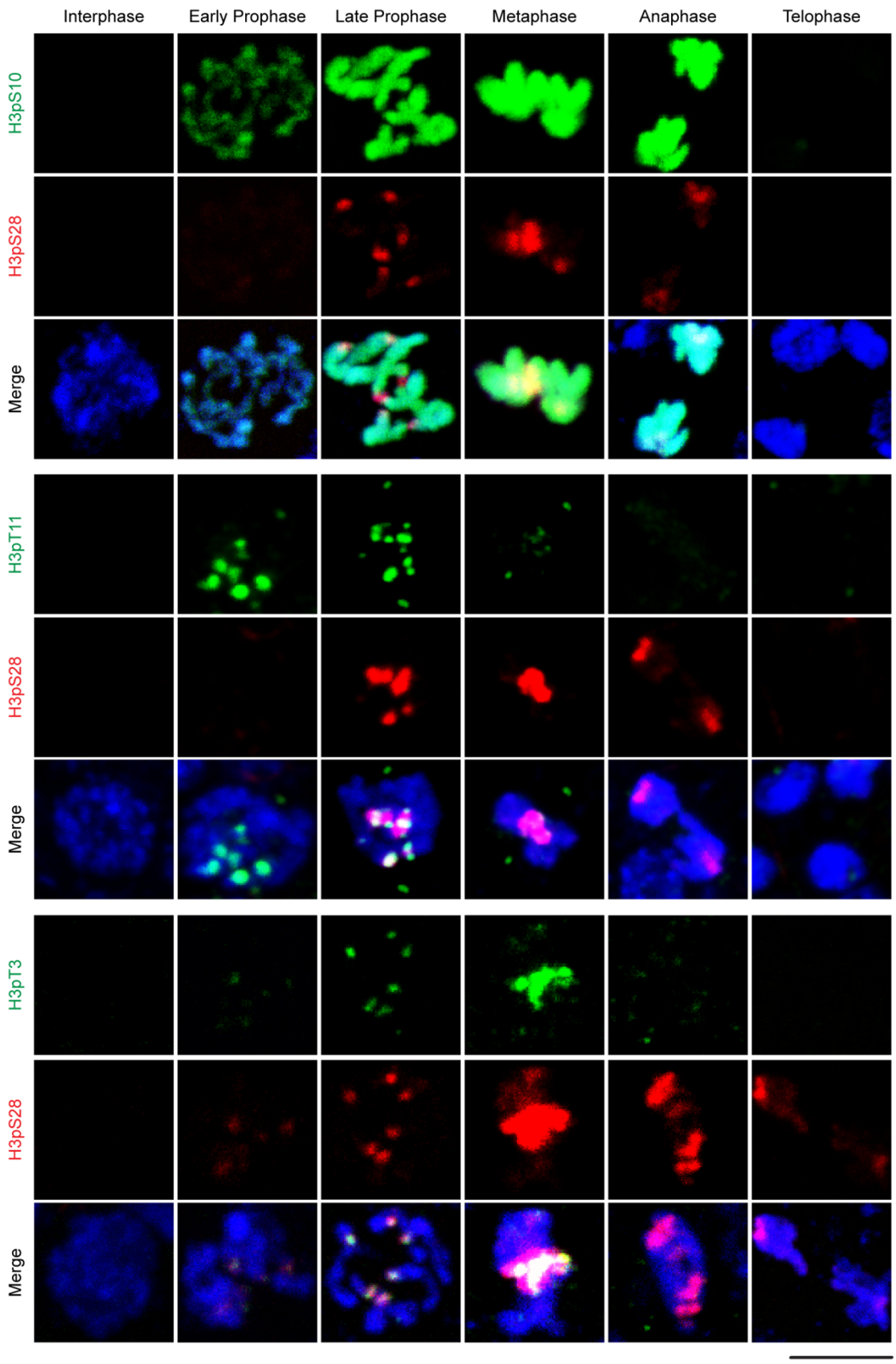
Interphase
Early Prophase
Late Prophase
Metaphase
Anaphase
Telophase
H3pS10
H3pS28
Merge
H3pT11
H3pS28
Merge
H3pT3
H3pS28
Merge

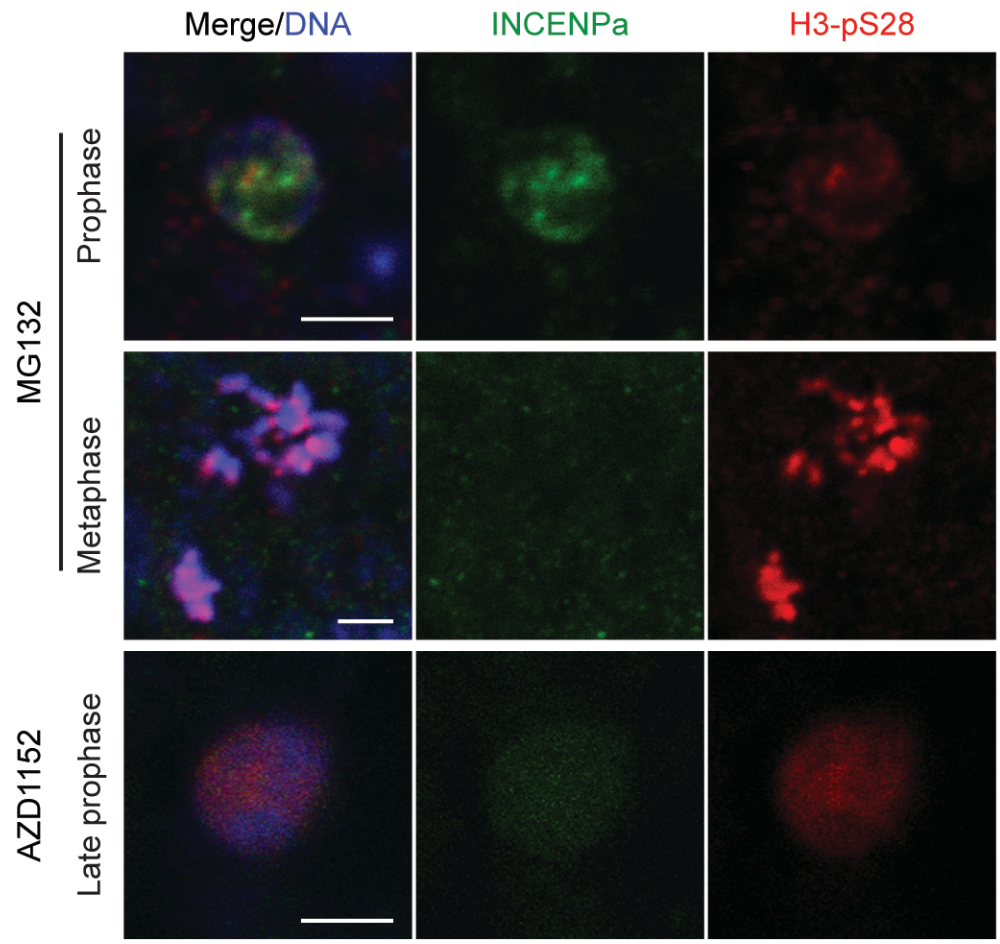

Figure S2. **Localization of the INCENPa paralog in mitotic cells in the presence of the proteasome inhibitor MG132 or the Aurora B inhibitor AZD1152**. INCENPa-GFP cmRNA injected embryos were incubated for 2 h in the presence of MG132 or AZD1152 and cells in mitosis were assessed for the localization of INCENPa-GFP. In the presence of MG132, as in untreated control embryos, INCENPa showed a pulsed enrichment on centromeres in late prophase but was absent from centromeres at metaphase, when H3pS28 reached maximum levels on centromeres, suggesting that loss of this centromeric INCENPa enrichment is not due to degradation of INCENPa, but rather its delocalization. AZD1152 treatment resulted in delocalized spreading of INCENPa and H3-pS28 on chromatin during late prophase, suggesting Aurora B activity is required for pulsed enrichment of INCENPa at centromeres in late prophase. Bars, 2 μm.

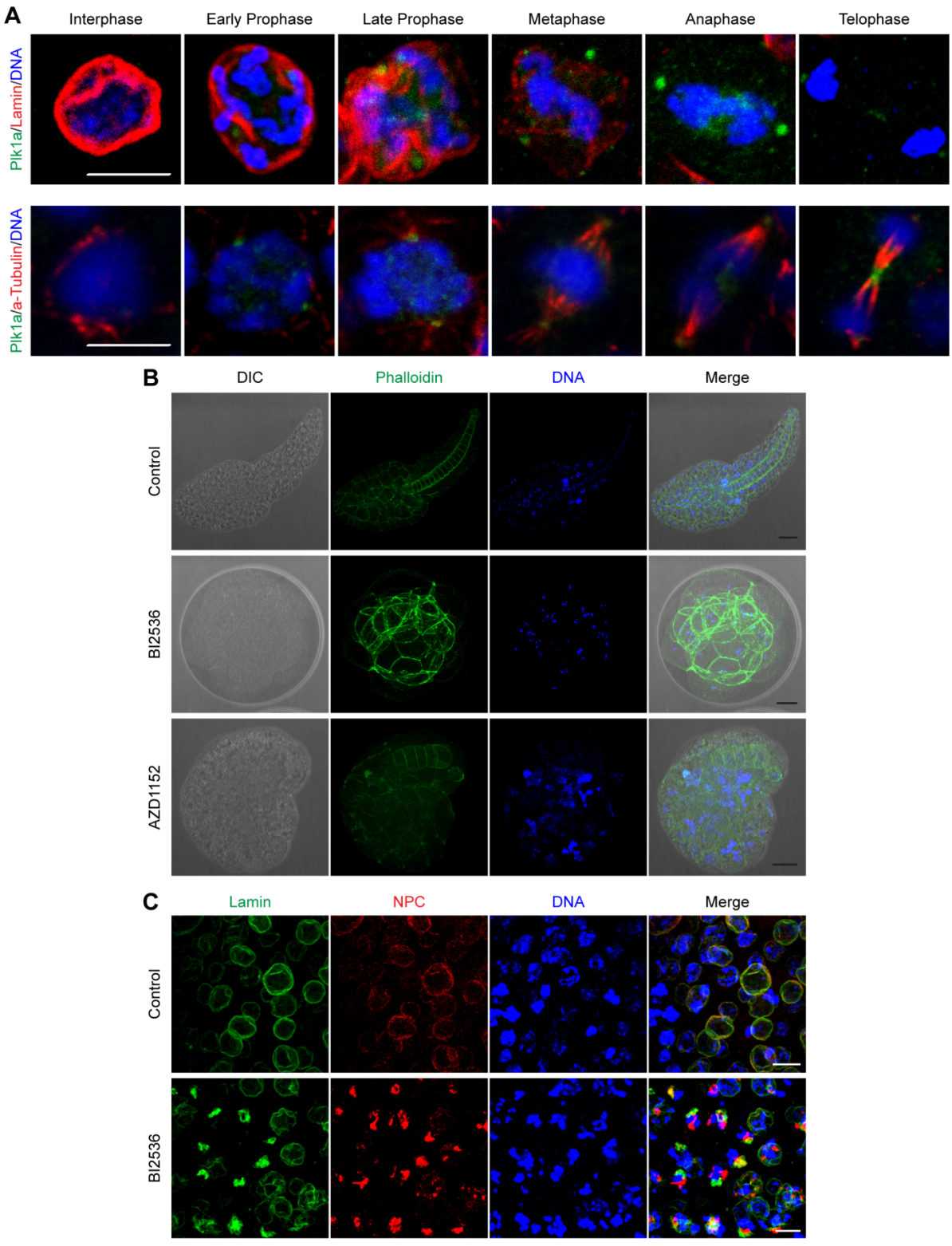

Figure S3. **Localization of Plk1a during mitosis and the phenotypes caused by its inhibition. (A)** Plk1a localized on centrosomes from early prophase, briefly enriched on

centromeres during late prophase, and localized to the central spindle during anaphase and telophase. Lamin staining follows the breakdown of the nuclear envelope and α-tubulin staining shows the mitotic spindle. Bars, 3 μm. **(B)** Inhibition of Plk1 (BI2536) caused rapid developmental arrest in early embryos. Inhibition of Aurora B (AZD1152) caused developmental arrest before hatching. Phalloidin staining of cortical actin indicates cell boundaries. Bars, 20 μm. **(C)** Inhibition of Plk1 caused defects in nuclear membrane disassembly. Mitotic nuclei with condensed chromatin retained association with lamin and nuclear pore complexes (NPC). Bars, 5 μm.

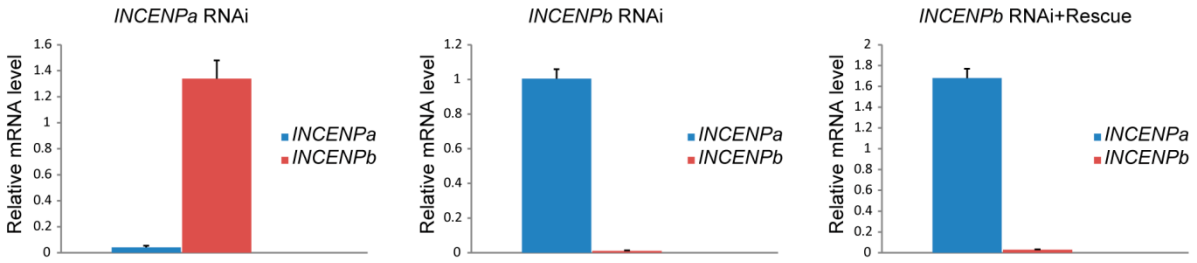

Figure S4. **Efficient knockdown of target gene endogenous mRNAs was verified by RT-qPCR in *INCENPa* RNAi, *INCENPb* RNAi and *INCENPb* rescue assays.** Knockdown efficiency of the target genes relative to wild type are shown as mean values (n=3) with SE.

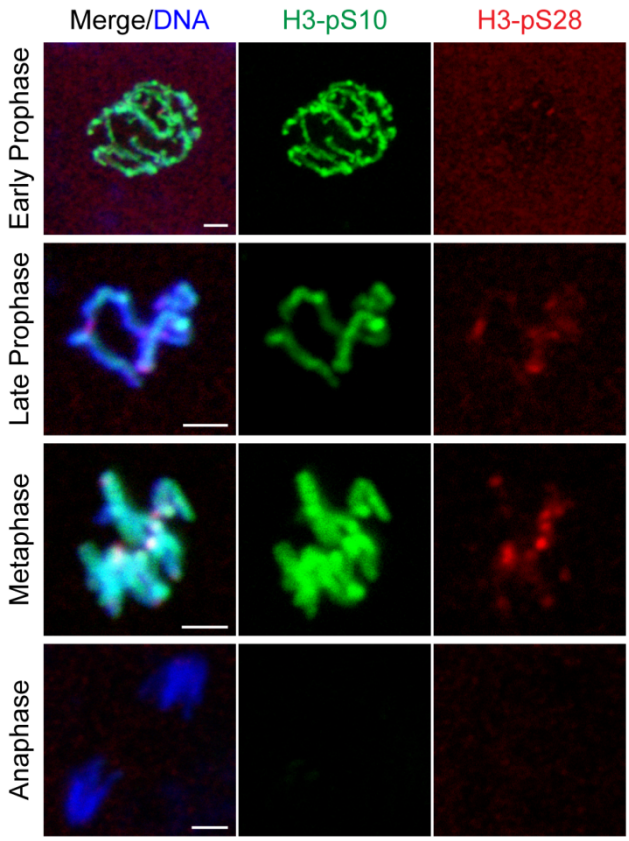

Figure S5. ***INCENPb*** **knockdown did not affect H3pS10 and H3pS28 staining in mitosis.** H3pS10 localized on entire chromosomes from early prophase, attaining a maximum level at metaphase. H3pS28 emerged on centromeres from late prophase and reached maximum levels at metaphase. Both H3pS10 and H3pS28 disappeared at anaphase. Bars, 2 μm.

Video S1. ***INCENPb*** **knockdown resulted in cleavage furrow regression during early embryonic divisions.** *INCENPb* knockdown oocytes extruded two polar bodies as normal after fertilization. During the first mitotic division, the formation and ingression of the cleavage furrow was executed with correct timing, but abscission was not completed and the cleavage furrow regressed. In subsequent attempted multi-planar divisions, the cleavage furrows repetitively regressed during mitotic exit, resulting in a multinucleate single cell at a time when control embryos gastrulated. Time-lapse video frames were recorded at 10s intervals from 5 min post fertilization until 2 hours post-fertilization. Video playback is at 6 frames per second.